Analytica Chimica Acta 760 (2013) 75–82

Contents lists available at SciVerse ScienceDirect

Analytica Chimica Acta

journal homepage: www.elsevier.com/locate/aca

Simple approach to study biomolecule adsorption in polymeric microfluidic channels

Vladimir Gubala[a,b,*,1], Jonathan Siegrist[a,1], Ruairi Monaghan[a], Brian O'Reilly[a], Ram Prasad Gandhiraman[a], Stephen Daniels[a,c], David E. Williams[a,d], Jens Ducrée[a]

[a] Biomedical Diagnostics Institute (BDI), National Centre for Sensor Research (NCSR), Dublin City University, Dublin 9, Ireland
[b] Medway School of Pharmacy, University of Kent, Central Avenue, Anson 120, Chatham Maritime, Kent ME4 4TB, United Kingdom
[c] National Centre for Plasma Science and Technology (NCPST), Dublin City University, Dublin 9, Ireland
[d] MacDiarmid Institute for Advanced Materials and Nanotechnology, School of Chemical Sciences, University of Auckland, Auckland 1142, New Zealand

HIGHLIGHTS

- A simple tool to assess biomolecule adsorption onto the surfaces of microchannels.
- Development for dilution by surface-adsorption based depletion of protein samples.
- It can easily be done using a readily available apparatus like a spin-coater.
- The assessment tool is facile and quantitative.
- Straightforward comparison of different surface chemistries.

GRAPHICAL ABSTRACT

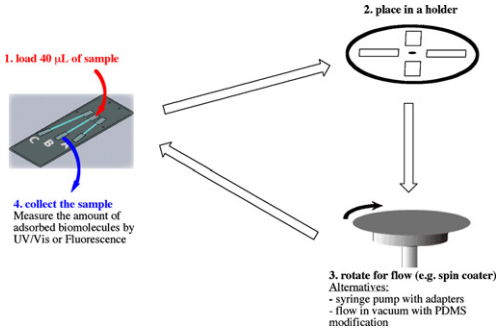

ARTICLE INFO

Article history:
Received 8 October 2012
Received in revised form
13 November 2012
Accepted 16 November 2012
Available online 29 November 2012

Keywords:
Antibody adsorption
DNA adsorption
Microfluidics
Polymer substrates
Zeonor®

ABSTRACT

Herein a simple analytical method is presented for the characterization of biomolecule adsorption on cyclo olefin polymer (COP, trade name: Zeonor®) substrates which are widely used in microfluidic lab-on-a-chip devices. These Zeonor® substrates do not possess native functional groups for specific reactions with biomolecules. Therefore, depending on the application, such substrates must be functionalized by surface chemistry methods to either enhance or suppress biomolecular adsorption. This work demonstrates a microfluidic method for evaluating the adsorption of antibodies and oligonucleotides surfaces. The method uses centrifugal microfluidic flow-through chips and can easily be implemented using common equipment such as a spin coater. The working principle is very simple. The user adds 40 L of the solution containing the sample to the starting side of a microfluidic channel, where it is moved through by centrifugal force. Some molecules are adsorbed in the channel. The sample is then collected at the other end in a small reservoir and the biomolecule concentration is measured. As a pilot application, we characterized the adsorption of goat anti-human IgG and a 20-mer DNA on Zeonor®, and on three types of functionalized Zeonor: 3-aminopropyltriethoxysilane (APTES) modified surface with mainly positive charge, negatively charged surface with immobilized bovine serum albumin (BSA), and neutral, hydrogel-like film with polyethylene glycol (PEG) characteristics. This simple analytical approach adds to the fundamental understanding of the interaction forces in real, microfluidic systems. This method

* Corresponding author at: University of Kent, Medway School of Pharmacy, Central Avenue, Anson 120, Chatham Maritime, ME4 4TB, Kent, United Kingdom. Tel.: +353 1 700 6337; fax: +353 1 700 5668.
E-mail address: V.Gubala@kent.ac.uk (V. Gubala).
[1] These authors contributed equally to the work and are considered co-first authors.

0003-2670/$ – see front matter
http://dx.doi.org/10.1016/j.aca.2012.11.030

provides a straightforward and rapid way to screen surface compositions and chemistry, and relate these to their effects on the sensitivity and resistance to non-specific binding of bioassays using them. In an additional set of experiments, the surface area of the channels in this universal microfluidic chip was increased by precision milling of microscale trenches. This modified surface was then coated with APTES and tested for its potential to serve as a unique protein dilution feature.

1. Introduction

Current requirements for biomedical point-of-use diagnostic devices create demand for inexpensive, single-use substrates, the ability to take measurements of complex biological samples with volumes ranging from microlitres to millilitres, and the need to operate in a sample-to-answer mode at minimum user intervention. As a result, the substrate utilized for microfluidic diagnostic devices is very often a polymer/plastic material.

Poly(methyl methacrylate) (PMMA) and cyclo olefin polymers (COPs) are prime examples of classes of polymer suitable as substrates for single-use diagnostic devices [1,2]. COPs are commercially available under various brand names, some of which are made from more than one kind of monomer and therefore also known as cyclic olefin copolymers (COCs) [3]. COP, in particular, has been engineered to meet key criteria such as high chemical resistance, low water absorption, good optical transparency in the near UV range, low autofluorescence, ease of fabrication (e.g., mouldability and machinability), and low non-specific adsorption of biomolecules. The two latter parameters are of particular importance. Specific to single-use lab-on-a-chip systems for bioassays, there is a need for microstructuring to incorporate various functional elements to pre-condition and handle a biosample, e.g., metering, mixing, dilution or concentration in an appropriate buffered solution, plasma extraction, filtration, purification, and the interaction with other bulk or surface-confined reagents [4–6]. Moreover, the chip design may include several measurement areas and controls to validate the assay. This can be achieved by incorporation of surface-immobilized biomolecular probes, microfluidic elements, and other functional components onto or into the substrate/chip [7].

The second requirement, low non-specific biomolecule adsorption, owes to the fact that the analyte of interest is usually present in the sample in extremely low quantities (e.g. in case of circulating tumour cells it is thought to be about 10 molecules per 1 mL; the clinically relevant concentration for antibody-based detection is typically in the range from fM to μM), especially as compared to other, non-analyte constituents. Furthermore, miniaturization itself implies notably enhanced surface-to-volume ratios and short diffusion distances compared to conventional laboratory methodologies. Thus, (rare) target molecules may be completely lost by non-specific adsorption at the walls of the channels and cavities along the upstream sample preparation, even before reaching the detection chamber. It is therefore absolutely critical to minimize surface adsorption while delivering the analyte through the microfluidic pre-processing features to the active assay area of the chip substrate. For typical diagnostic analytes containing low concentrations of antibodies or nucleic acids (the typical clinical concentration range is between pg mL^{-1} and ng mL^{-1}) sample preconditioning in these "lossy" fluidic networks would distort quantitation and even create false negatives.

A repertoire of surface chemistries has been reported for pristine plastic materials to suppress non-specific adsorption [2,8]. However, to the best of the authors' knowledge, there is no readily available analytical technique to characterize biomolecular adsorption occurring upon passage of samples through chemically modified microfluidic channel networks.

Table 1
Basic equations for the centrifugal flow and characteristic timescales governing adsorption on the channel walls. The force due to the capillary pressure is assumed to be significantly less than the centrifugal pressure. If ρ denotes fluid density, ω denotes angular velocity, η denotes viscosity, $\bar{r}$ the mean radial position of a liquid plug and d the diameter of a (round) radial channel, then $\bar{v} = (\rho/32\eta)\bar{r}d^2\omega^2$ provides the average velocity of the centrifugal flow. This is used as an approximation for the rectangular channel, with d representing the height of the channel. The characteristic timescales will follow these simple equations where Δr represents the (radial) length of the channel, k_{on} rate constant for adsorption, k_{off} rate constant for desorption. The rate constants depend upon the actual area, taking into account the roughness of any surface coating.

Residence timescale for fluid in the channel at radius, $\bar{r}$	$\tau_{fluid} = \frac{\Delta r}{\bar{v}} = \frac{32\eta\,\Delta r}{\rho\bar{r}d^2\omega^2}$
Residence timescale of material on surface	$\tau_{surface} = \frac{1}{k_{off}}$
Timescale to approach saturation of surface	$\tau_{sat} = \frac{1}{k_{on}c+k_{off}}$

In this work, a novel method is presented to facilitate the rapid characterization of conformal surface chemistries and their interactions with biomolecules under the specific, high surface-to-volume ratio conditions governing microfluidic lab-on-a-chip systems. In particular, the biomolecule (viz., antibody or DNA) adsorption properties of surface coatings deposited using plasma-enhanced chemical vapour deposition (PECVD) are examined using the microfluidic chips as tools towards the development of diagnostic systems. The current state-of-the-art in the manufacture of plastic, disposable devices with incorporated microfluidics features requires the use of more than one piece of polymer, usually bonded together by pressure sensitive adhesive. The manufacture of the chips is becoming fully automated, which further improves the reproducibility and the performance of the devices. The design of our microfluidics chip (Fig. 1) was therefore chosen to be also made from multi-layered material to resemble the variables of the real platforms as closely as possible. Absorption conditions are 'microfluidic' in a way that the channel height was set to 50 μm, i.e. a laminar "gap" flow. This way, the maximum diffusion distance to the wall, which is relevant for surface adsorption, is 25 μm, only. We note that our analytical method is also amenable to more narrow channels or channels with different geometry.

As a pilot study, we have chosen to functionalize polymer substrates by an established, automated and commercially viable PECVD processes. However, the analytical method presented is by no means limited to this particular surface chemistry technique or surface/substrate type. Any other standard substrate (e.g. glass, silicon, plastic, noble metal films, etc.) and surface chemistry approach (standard wet chemistry approaches, self-assembled monolayers, vapour deposition methods, etc.) would be easily incorporated into the device by coating of the polymer layers before assembly.

For a reasonable qualitative explanation of all the observations discussed in this article, we established simple theoretical calculations on the timescales. Table 1 sets out some basic equations describing the centrifugally driven flow in the channel and sets out the characteristic timescales that govern flow and adsorption.

Consideration of the timescales gives the following simple design criteria:

- If $\tau_{fluid} \ll \tau_{sat}$ then very little material will be adsorbed.

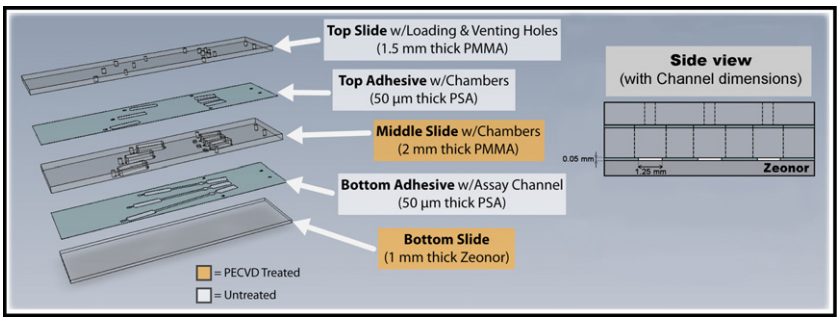

Fig. 1. Schematic showing the 5 layers of the slide-sized microfluidic characterization system. The microfluidic channel is laterally defined by cutting the bottom pressure-sensitive adhesive (PSA). The system provides modularity as the bottom slide can consist of any material desired (e.g., glass) and the layout of the chip can be easily altered.

- If $\tau_{sat} \ll \tau_{fluid}$ then the entire surface of the channel will be saturated after a short time.

If the surface is not close to saturated over its entire length, then:

- If $\tau_{surface} \ll \tau_{fluid}$ then the adsorbate will be uniformly distributed down the channel.
- If $\tau_{surface} \gg \tau_{fluid}$ then the adsorbate will move in a front down the channel, as the surface saturates.

Therefore the position of the front will depend upon the binding capacity of the surface (amount adsorbed per unit geometric area at saturation).

In this paper, we introduce a simple and low-cost testing scheme to investigate flow-rate dependent protein (IgG) and DNA adsorption in microchannels machined in a commonly used COP (Zeonor®) substrate having both native and coated polymer surfaces. Coatings of aminopropyltriethoxysilane (APTES), bovine serum albumin (BSA)-treated APTES, and diethylene glycol dimethyl ether (PEG) are investigated. The microfluidic chip, based on a standard microscope slide format (75 mm × 25 mm), was fabricated using simple and inexpensive materials and methods accessible to the overwhelming majority of research groups. The modular fabrication permits to screen a broad range of (functionalized) substrate materials. The flow velocity is controlled in a jitter-free fashion by centrifugal microfluidic actuation by a low-cost spindle motor, which may even be substituted by a simple spin coater, which allows for easy variation of the fluid residence time through the angular velocity ω. We note that the flow generation in the presented microfludics chip is by no means limited to centrifugal actuation. The versatility of modified PMMA cells with appropriate connectors was recently demonstrated in our group using a standard syringe pump [9] and modifications exploiting vacuum or pressure-driven flow can be used as well [10].

In the final part, a microfluidic device with the miniaturization-related, increased surface-to-volume ratio is examined for potential for use as a unique protein dilution feature.

2. Experimental

2.1. Microfluidic chip design and fabrication

Phosphate buffered saline (PBS, pH 7.4, 0.01 M), bovine serum albumin (BSA, 98%), 3-aminopropyltriethoxysilane (APTES), diethylene glycol dimethyl ether (DEGDME, $CH_3O(CH_2CH_2O)_2CH_3$), and Cy5-IgG were all purchased from Sigma–Aldrich (Dublin, Ireland). ssDNA (20-mer) with a 3′-C_6-NH_2 modifier and a 5′-Cy5 label was purchased from MWG Biotech (Ebersberg, Germany). All chemicals were used as received without further purification.

The microfluidic chip in Fig. 1 was designed using AutoCAD (AutoDesk, US) and consisted of a total of 5 laminated layers of laser-cut polymethylmethacrylate (PMMA) (#824-632 & #824-480, Radionics, IE), knife-cut, double-sided, pressure-sensitive adhesive (PSA) (ARcare 8890, Adhesives Research, IE), and Zeonor® substrates (Fig. 1). Injection-moulded Cyclo olefin polymer (COP) slides (Zeonor® 1060R, 25 mm × 75 mm, 1 mm thick) were obtained from Sigolis (Uppsala, Sweden). The PMMA layers were laser-cut using a relatively inexpensive benchtop tool (Epilog Zing, Epilog, US) and the PSA layers were structured using a benchtop knife-cutter (Craft Robo-Pro, Graphtec, UK). In all cases, the AutoCAD drawing layers were easily imported into the software for the respective pieces of fabrication equipment.

All polymer chip components (including the bottom Zeonor® substrates) were ultrasonically cleaned before assembly and/or PECVD coating. After PECVD-coating of the middle (PMMA) and Zeonor® bottom parts, which consisted of the roof and floor of the microfluidic channels, respectively, the layers were manually assembled using alignment pins. Finally, the completed parts were rolled under pressure to ensure excellent adhesion between the polymer and PSA layers. This is similar to methods already reported in the literature for fabrication of polymer microfluidic devices [11,12].

2.2. Coating of COP substrates by plasma enhanced chemical vapour deposition (PECVD)

The measured substrates were coated by a PECVD technique as described previously [8,13]. Briefly, the functional coatings were carried out in a computer controlled PECVD reactor Europlasma, model CD300 (Oudenaarde, Ghent, Belgium). An aluminium vacuum chamber, connected to a Dressler CESAR 136 RF power source (Munsterau, Stolberg, Germany) with an operating frequency of 13.56 MHz, with an automated impedance-matching box, was used. APTES or DEGDME were contained in two separate single side blocked KF16 nipples (Kurt J Lesker, UK) connected to the chamber individually through needle valves. The needle valves were used to control the flow of vapours of the precursors. Plasma pretreatment was carried out at an RF power of 250 W for 3 min with 50 sccm of argon flow and 50 sccm of oxygen flow. The plasma deposition was carried out in argon plasma. The COP substrates were placed at a floating electrode and the input power was fixed at 14 W. For the BSA-coated slides, the APTES coated substrates were immersed for 1 h in a 6% (w/v) solution of bovine serum albumin (BSA) in PBS buffer at pH = 7.2.

2.3. Water contact angle and thickness measurements

The film wettability was analysed by measuring the water contact angle using the First Ten Angstroms FTA200 (Portsmouth,

VA, USA) contact angle analyzer. A high purity HPLC grade water (Sigma–Aldrich, Dublin, Ireland) was used for the measurements. Images of drops were recorded with a CCD camera and analysed using the accompanying software. The thickness of the films deposited on the sensing substrate was measured by an UVISEL spectroscopic ellipsometer (Jobin Yvon Horiba, France) in external mode. A three-layer model (BK 7 glass, Au and add layer) was used in the fitting with PsiDelta 2 software (Jobin Yvon Horiba, France) to obtain the thickness of each layer from the measured Ψ and Δ spectra.

2.4. Centrifugal pumping and imaging

To run the centrifugal microfluidic experiments, a servomotor coupled to a stroboscopic visualization system similar to that already described in the literature [14] was used for tracking of flow during rotation. A servomotor (4490 series, Faulhaber, DE) was mounted to a framed support, and a chuck was machined for securely attaching a centrifugal slide-holder template to the shaft of the motor. A CCD camera (Sensicam series, PCO, DE) was placed directly above the motor, and a combination of optical components (Navitar, NY, USA) were attached to the camera to obtain an image with motorized zoom and focus controls for flow visualization; various optical configurations allowed for microscopic and macroscopic imaging of features on the microfluidic devices. A linear drive was used to radially position the camera along the centrifugal slide-holder.

The camera was triggered to capture one frame per rotation, such that a movie composed of a sequence of still images taken at the same location on the device(s) could be acquired (Fig. 2b). A custom control box was built to manage trigger signals between the motor, the camera, and the stroboscopic illumination; the trigger box also controlled the azimuthal position along the centrifugal slide-holder for image acquisition. The combined action of the linear-drive mounted camera, the trigger box and optical setup allowed surveying the fluidics at any arbitrary sector of the disc. The stroboscope (Drelloscop 3244, Drello, DE) utilized a liquid light-conductor for illumination and was mounted to the side of the camera. A desktop PC (Dell, US) controlled the spin-speed of the motor as well as the monitoring and acquisition of the images. The custom spin-stand instrument enabled real-time movement and magnification of the image acquisition such that flow through the microfluidic devices could be tracked. The optical clarity of the acrylic and adhesive device components provided adequate contrast for visualization.

2.5. Flow characterization

Contrast agent (<1%, v/v) was added to phosphate buffered saline (PBS, pH 7.2) and loaded onto the devices using a standard pipette to monitor the flow through the microfluidic device. Mock 40-μL samples where then centrifugally pumped through the system at various spin-speeds (specified in revolutions-per-minute, RPM) and timed to determine approximate flow rates.

2.6. Enhancing surface area

For the devices with increased surface area, the surface was modified by a 3-axis micromilling machine (CAT3D M6, Datron AG, Germany). The channel surface was machined with a 100-μm tool at 16,000 RPM using a 0.9 mm s^{-1} feed rate. The trace was drawn using Excalibur CAD/CAM package (Excalibur XCAD 4.201, Progressive Software Corporation, USA). The trace produced a 100-μm wide and 80-μm deep channel, with each channel separated by a 50-μm wall. Across the channel width of 1.25 mm, the machining produced eight, 80-μm wide troughs.

2.7. Surface chemistry characterization

To test the coated surface chemistries on the microfluidic devices, 4 chips were placed onto the same centrifugal slide-holder. The 40-μL samples were prepared in PBS buffer and consisted of Cy5-labelled goat anti-human IgG at 4.0 μg mL^{-1} and Cy5-labelled ssDNA at 5.0 nM.

The liquid samples were loaded onto the chips, the extraction holes sealed using adhesive tape, and the samples centrifugally pumped through the system at spin-speeds ranging from 300 RPM to 400 RPM. The samples were then removed using a pipette, loaded in a standard 96-well plate and the fluorescence intensities were analysed on a Safire (Tecan) microplate reader. For the Cy5-labelled materials, the excitation and emission wavelengths were set at 646 nm and 662 nm, respectively.

3. Results and discussion

3.1. Microfluidic operation, ease-of-use, and advantages

The device design consisted of deep chambers that can accommodate real-world sample volumes from 1 μL up to 40 μL. The microfluidic channel itself was 1.25 mm wide and only 50 μm deep, as set by the total thickness of the (cut) PSA, to enable analysis of the surfaces under microfluidic conditions. The thickness of the microfluidic channel can easily be changed by selecting a PSA with a different (commercially available) film thickness.

The particular design presented in Fig. 2 consisted of three separate channels, A, B and C, each of a different length (A: 13 mm, B: 18 mm, C: 23 mm), see also Table 2. This geometrical variation enabled an analysis of how the surface area affects the adsorption of biomolecules.

A manifold of geometrical designs can be realized, e.g., by adapting the width, height, aspect ratio and length of each channel. Finally, whether using centrifugal- or pressure-driven flow, the flow rate can be varied to enable additional analysis parameters. In the development of microfluidic diagnostic devices, the interaction of surface chemistries tends to be very sensitive to the specific surface-to-volume ratios and convection–diffusion conditions of strictly laminar flow. They can critically differ from the conditions prevailing in stagnant well-plate or test-tube found in standard benchtop assays. The system presented allows for facile analysis of surface chemistries under microconfinement as is required during the development of microfluidic diagnostic devices.

3.2. Flow analysis

The spin-speeds used to test the native COP, APTES, PEG, APTES + BSA, and microstructured APTES surfaces were kept constant at 300 RPM (400 RPM for the pristine COP due to its hydrophobicity). The more hydrophilic surfaces, such as PEG, APTES, APTES + BSA, required a slightly lower spin-speed while the pristine COP surfaces, being more hydrophobic, required a slightly higher spin-speed to initiate and maintain flow (for water contact angles and of the film thicknesses, see Fig. 3). In all cases, the flow-rates achieved were approximately 0.3 μL s^{-1}. Some variability was observed, likely arising from anomalies due to the quality of surface coatings and manual chip fabrication. Fig. 2 shows a sequence of movie frames from sample loading to completion of centrifugal flow-through.

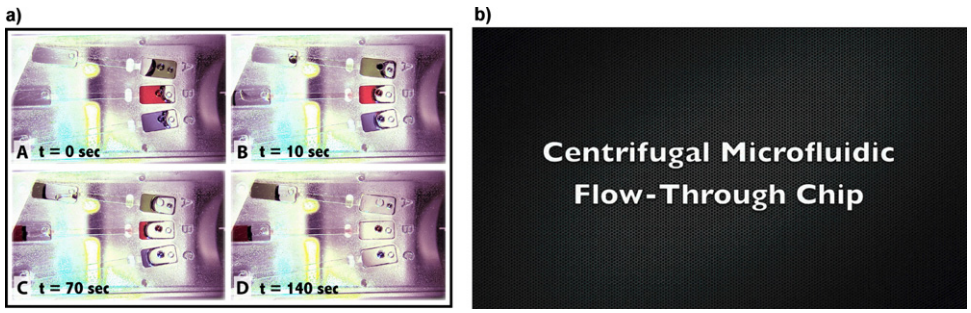

Fig. 2. (a) Photos showing the various stages of microfluidic pumping (device loaded with contrast dyes). (A) Samples loaded, (B) commencement of flow as the device spins, (C) continuing flow, and (D) samples after passing across the coated surfaces and ready to be removed for analysis. The capillary burst valves at the exit of the inlet chambers avoid priming during the loading phase and synchronize the release into the adsorption channel. The channel dimensions are listed in Table 2. (b) A movie showing the operational mode of the microfluidic device (enhanced online).

Table 2
Dimensions of the 1.25-mm wide and 0.05-mm high channels with the maximum theoretical amount of IgG and ssDNA adsorbed per channel.

	Channel A	Channel B	Channel C
Length	13 mm	18 mm	23 mm
Flat/total surface area	33.8 mm^2/67.4 mm^2	46.8 mm^2/93.3 mm^2	59.8 mm^2/119.2 mm^2
Theoretical maximum of IgG per channel[a]	0.3×10^{-12} mol, 0.048 μg	0.4×10^{-12} mol, 0.064 μg	0.5×10^{-12} mol, 0.080 μg
Theoretical maximum of ssDNA per channel[a]	2.0×10^{-12} mol, 13.2 ng	2.8×10^{-12} mol, 18.5 ng	3.5×10^{-12} mol, 23.1 ng

[a] Assuming a maximum of 50% coverage.

3.3. Adsorption of proteins and DNA on microchannel substrates

In this work, the antibody and DNA adsorption on four different surface coatings was studied. The first coating was prepared by PECVD deposition of APTES, an amine-functionalized siloxane. We have previously reported on the preparation and characterization of such films by a number of analytical methods [15]. The APTES-film thickness, as a result of plasma assisted polymerization process, depends on the deposition conditions and can range between 5 nm and 20 nm. Considering that the pK_a of APTES is around 10, the surface is predominantly positively charged upon contact with the PBS solution (pH = 7.2). The second coating was rendered negatively charged by immersing APTES-coated substrates into a 6% (w/v) solution of BSA [16]. BSA is commonly used as a biological blocking agent and it can be adsorbed on positively charged surfaces in monolayers, bilayers or even multilayers depending on the deposition conditions such as the concentration, pH, time and ionic strength of the solution [17,18]. In either case, the net result is an effective increase of the negative charge at the interface between the biomolecule and the surface. The thickness of the film after the BSA deposition is increased by 3.5 nm (Fig. 3),

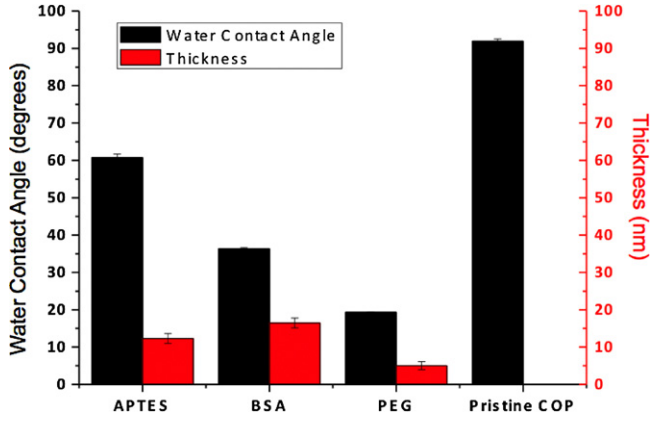

Fig. 3. Thickness (measured by ellipsometry) of films prepared by PECVD and their corresponding water contact angles ($N = 3$, error bars are ±1 standard deviation).

suggesting that the BSA was adsorbed in a monolayer on the APTES treated COP slide (considering the Stoke radius of BSA is ~3.4 nm [19]). The PEG precursor used in the third type of surface possessed no charge. While plasma assisted deposition could have fragmented its native structure and formed a small number of ions and reactive radicals, this surface can be considered to be close to neutral, especially when compared to the charged APTES and BSA films. The fourth studied surface was a pristine, unmodified COP (Zeonor®) slide. The differences in chemical groups exposed to the measured samples are illustrated schematically in Fig. 4.

The substrate adsorption characteristics of the Cy5-labelled IgG antibodies and DNA are presented as percentages of capture efficiencies for each corresponding channel length. The values were simply calculated as the fraction of the molecules collected (once they finished flowing across the coated surfaces) to the starting molecule concentration. The results are summarized in Fig. 5.

IgG antibodies adsorbed well on the positively charged APTES surface, while the PEG and BSA-modified films reduced IgG binding significantly. In terms of the characteristic timescales, clearly, for the PEG surface, $\tau_{fluid} \ll \tau_{sat}$. For the APTES and BSA surface, the dependence on channel length shows that $\tau_{fluid} \sim \tau_{sat}$, with τ_{sat} for BSA being greater than that for APTES. The most efficient film in terms of suppressing non-specific adsorption was the PEG layer. The repulsion of proteins by PEG-like materials observed in this study is in good agreement with previous work [20]. This group has recently reported that PECVD-prepared PEG films exhibit roughness increases and significant swelling occurs upon contact with water; such surfaces become very well hydrated and resemble the structure of hydrogels.

The three channels differ in length and hence in surface area available for adsorption. The theoretical amount of antibody (assuming its surface footprint is ~100 nm^2) and DNA (~14 nm^2 for DNA 20-mer) [21] that can be realistically adsorbed on the channel surface was calculated. It was assumed that both IgG and DNA would adsorb as monolayers and would pack on the surface, effectively covering a maximum of 50% of the available area. These theoretical values are summarized in Table 2.

The amount of antibody adsorbed in the channels was in all cases proportional to their length, with the exception of the pristine COP. The hydrophobic pristine COP showed large variations in its

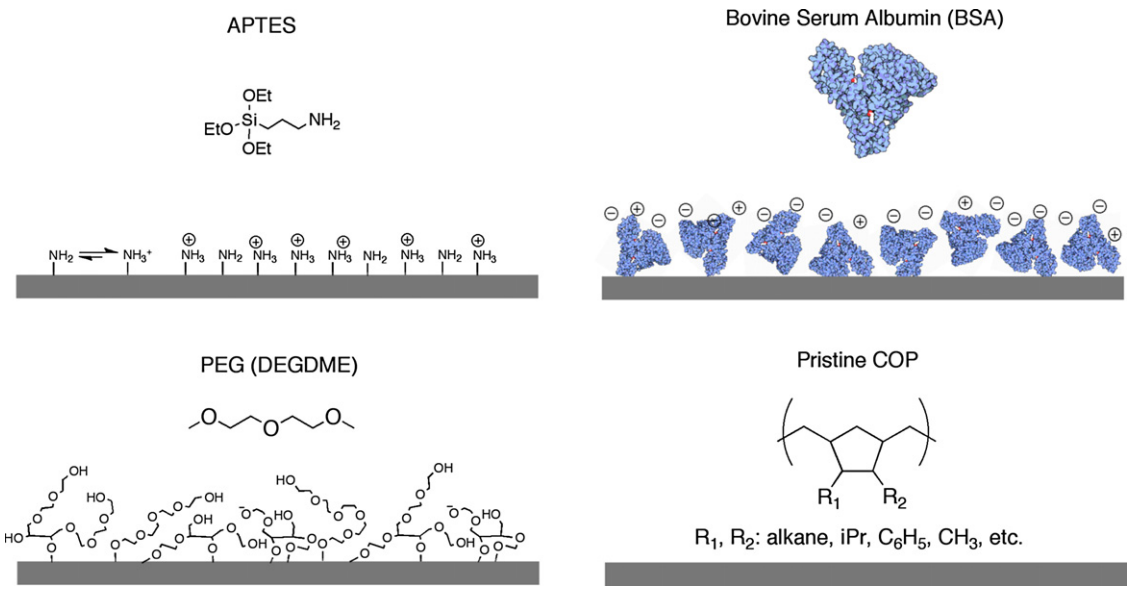

Fig. 4. A schematic of functional groups present at the biomolecule-surface interface on the four coatings characterized in this study.

adsorption capacity for antibodies. It is speculated that the antibodies can adsorb on the COP only if they change their native conformation, exposing some of their hydrophobic residues and allowing for effective π–π and van der Waals interactions with the unmodified COP surface. It is reasonable to assume that the timescale of such events is longer than the exposure time of the antibody solution during the flow, which impairs the reproducibility between individual experiments. The fact that native properties of the COP cannot be relied upon to satisfactorily inhibit non-specific adsorption is a practically highly relevant outcome for the design of a diagnostic device. Indeed, a specific surface coating is necessary to consistently prevent non-specific biomolecule adsorption.

Similar trends were observed when using ssDNA. The intrinsically negatively charged oligonucleotide showed very good adsorption on the positively charged APTES and exceptionally low adsorption on the negatively charged BSA surface. The fact that the neutral PEG film was not as effective at reducing non-specific binding of charged DNA molecules confirmed that the dominant forces behind the binding phenomena are the electrostatic interactions. In order to study the consequences of the adsorption phenomenon and the fluorescence contribution from the dye itself, hydroxylamine-quenched Cy-5 NHS ester dye was flown through the channels (Figure S1, Supporting Information). The effects of the dye adsorption on the BSA and pristine COP surfaces were negligible. However, the positively charged APTES surface showed some trend of low level Cy5 adsorption. This can be attributed to the charge factor. The Cy5 has two negatively charged sulphonate groups, which can be involved in non-covalent interactions with the positively charged amines of the APTES surface. Although the adsorption of the Cy5 dye was still much lower than the one observed for the Cy5 labelled IgG and DNA molecules, it follows the trend of an increase in fluorescence with increasing channel length. We also note that because each measurement takes only few minutes, no obvious photobleaching effect of the dye was observed.

The effect of adsorption efficiencies of antibodies upon varying the centrifugal speed rates was investigated as well. For this experiment, Cy-5 labelled anti human IgG on APTES coated chips was chosen, mainly because of the good affinity of IgG to the amino-functionalized surface and the clear, distinguishable difference between the channels A, B and C (Fig. 5A). As seen in Fig. 6, little difference in the antibody binding was observed at speeds up to 600 RPM. However, as expected, the molecular adsorption at 1500 RPM was significantly lower. The characteristic timescale for fluid flow, τ_{fluid} varies as $1/\omega^2$. This strong dependence is reflected in Fig. 6, where the adsorption is minimal at 1500 RPM ($\tau_{fluid} \ll \tau_{sat}$)

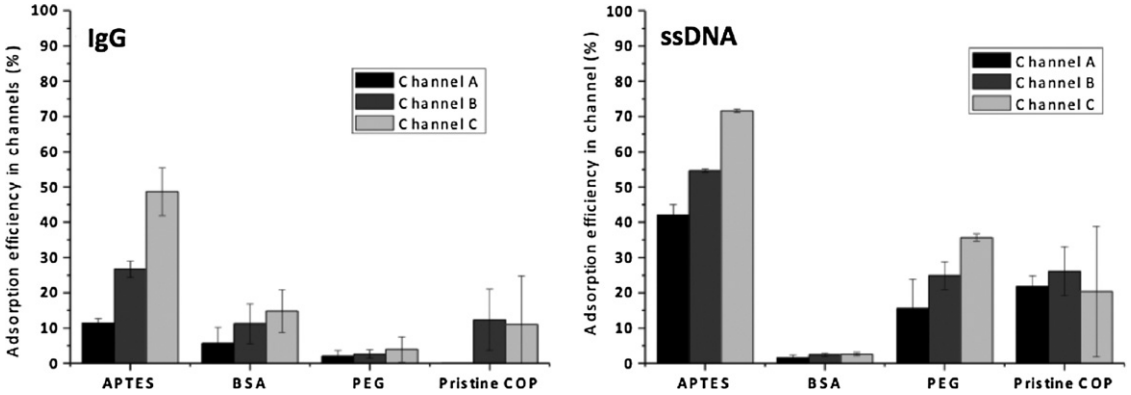

Fig. 5. The adsorption efficiency (calculated as $(1 - C_s/C_0) \times 100\%$, where C_s denotes the concentration of molecules after passing through the channel and C_0 denotes the initial concentration used before passing through the channel) of IgG antibodies and ssDNA on COP slides treated with various surface chemistries ($N = 3$, error bars are ±1 standard deviation). The channel geometries are compiled in Table 1.

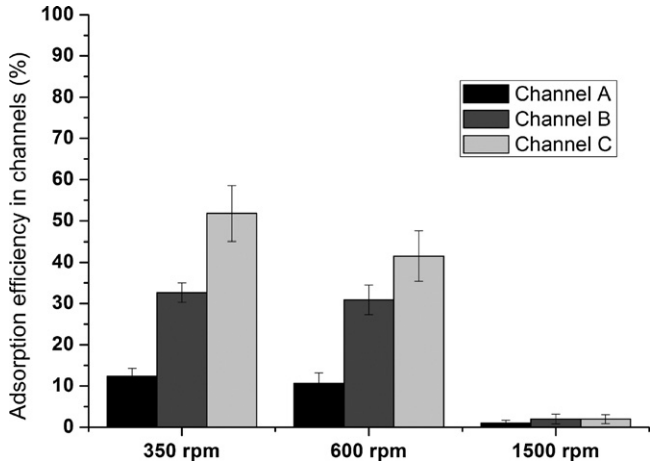

Fig. 6. The capture efficiency of the goat anti-human IgG antibodies on APTES coated chips at three different centrifugal speeds.

but significant, and dependent on channel length, for the lower rotation rates, implying that, for these, τ_{fluid} becomes greater than τ_{sat}. In principle, the movement of the adsorption front could be used to assess the rate constants for adsorption and desorption, but we were unable to do this since the chip was too thick to allow accurate imaging. Through a smart fluidic chip design, this flow-speed dependent effect may be explicitly utilized to simplify chip fabrication: instead of using different coatings to suppress adsorption in sample prep and stimulate surface interaction in the detection chamber, we flow rapidly through the upstream section and run the surface reactions in the final chamber in stopped, batch mode.

So far, these simple microfluidic chips proved to be useful in the assessment of adsorption of antibodies and nucleic acids on various surfaces. However, we envision that the same concept can be used in situations where, prior to detection, sample dilution is required. Common dilution designs rely on mixing of a fraction of the analytical sample with a precise volume of buffered solution [22–24]. This turns out to be somewhat challenging when considering the available surface area of the substrate and the fact that the buffers must be stored on the biochip, including valves for accurately releasing and dispensing the desired volumes. Moreover, the on-chip diluted solution should be homogeneous to ensure maximum reproducibility. Therefore, to test the potential of the microfluidic device presented in this article in a dilution experiment, goat anti-human IgG was subjected to APTES-coated channels with an enhanced surface area introduced by micromilling. The normally flat COP slides were milled with trenches that were 100 μm wide, 80 μm deep, and with 50 μm spacing along each channel.

The adsorption efficiency results, presented both in Figs. 5 and 6, do not show the ideal linearity trend and do not extrapolate to zero. This can be partially associated to the fact that the measurements were not performed under 'ideal' conditions. Instead, the design of the chip is set to simulate more realistic environment of modern microfluidics detection platforms. This includes many variables and challenges, most of which are presently unavoidable in the current chip manufacture processes or methods used for the surface functionalization.

As seen in Fig. 7, the capture efficiency, measured as a ratio/percentage between the concentration of adsorbed molecules in the channel and the initial concentration used in each channel, increased in the channels that were featuring milled trenches prior to deposition of APTES. Interestingly, the effect was more noticeable in the shorter channel A than in the longer channels B or C. Given that the adsorption of biomolecules onto a plastic surface is quite a complex process, such discrepancies in the capture efficiency can be attributed to several factors. Some are related to the poor control and resolution of the nanoscale surface finish of the micromilling process, which is important when considering

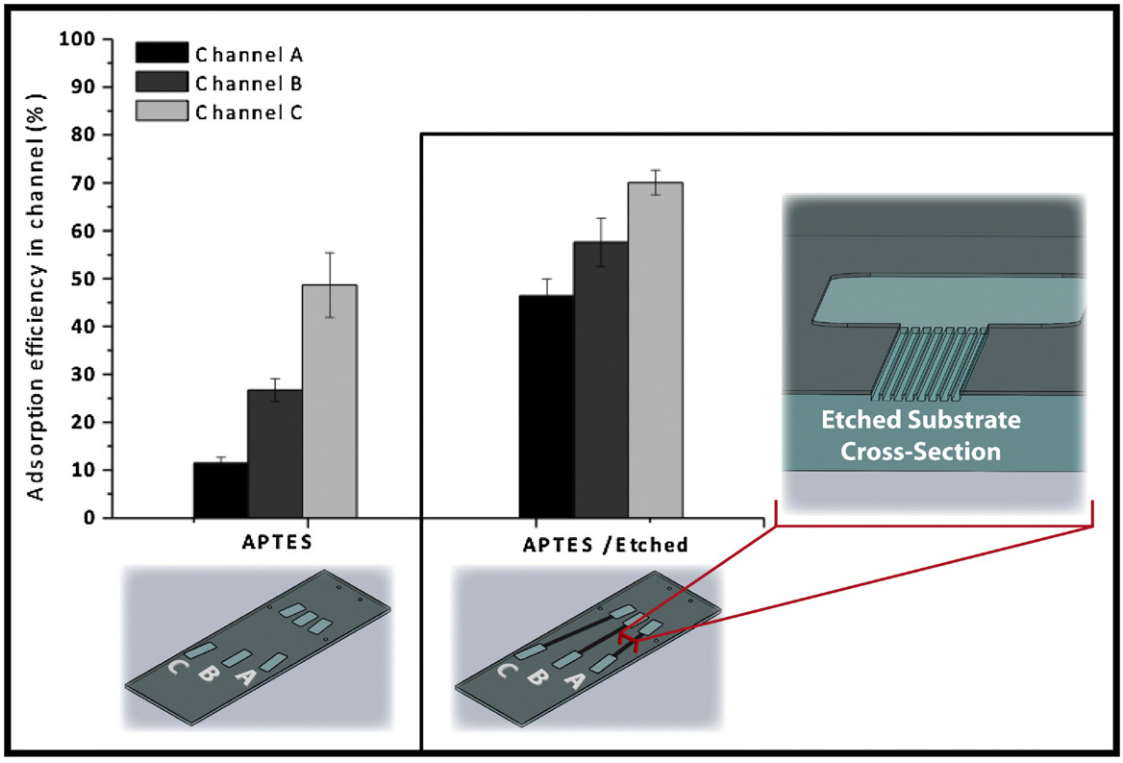

Fig. 7. The capture efficiency of the goat anti-human IgG antibodies in flat and trenched channels (100 μm wide, 80 μm deep, and with 50 μm spacing) subsequently coated with APTES. The channel geometries are compiled in Table 2.

the surface footprint of an antibody (~100 nm^2). Another factor relates to the uniformity of the deposited layer of APTES. We also surmise that varying convection–diffusion conditions at different flow rates have an impact on the adsorption kinetics and thus the eventual dilution ratio. Nonetheless, this novel, proof-of-concept dilution experiment showed about a 5-fold concentration increase of the adsorbed material on the micro-milled surface when compared with the flat, unmodified substrate. Currently, this may seem insufficient to replace the conventional valves and mixing chambers, which are used as reliable dilution elements. However, the presented data suggest that improvements in surface chemistry and more precise control over the surface area by introduction of trenches, pillars [2], or microbeads in the microchannels could increase the effect on adsorption and this may become a useful approach for microfluidic sample dilution.

4. Conclusions

The presented microfluidic chip represents a simple-to-use, inexpensive and available option for the analyses of both the specific and non-specific adsorption for any desired combination of surface composition and dissolved biomolecule. Typical convection–diffusion timescales governing adsorption in microfluidic channels can straightforwardly be defined and changed by altering channel geometries and the rotational frequency, which itself is conveniently controlled using a spin-coater. We have experimentally compared three different surface chemistries applied to the Zeonor® (COP) with respect to the adsorption of antibodies and DNA.

The microfluidic device presented here for the characterization of biomolecular absorption in microchannels excels with its ease of fabrication and layer-based modular assembly, thus lending itself to facile customization. We have also demonstrated its compatibility with many established lab protocols and systems, and its capacity to analyse many types of commonly used substrates. This makes the presented system a powerful and available approach for optimizing standard and customized surface chemistries.

We have also demonstrated a direct means for dilution of protein solutions in a microdevice. The key is observation of the passage of an adsorption front down a channel under the influence of centrifugal force. Although the results obtained in this pilot study are encouraging, it is obvious that further improvements and optimizations in the surface area, film uniformity, flow rates and the related convection–diffusion conditions are necessary to ensure reliable and accurate protein dilution in microfluidic devices.

Acknowledgments

This material is based upon work supported by the Science Foundation Ireland under Grant No. 10/CE/B1821. D.E. Williams is an E.T.S. Walton Visiting Fellow of Science Foundation Ireland.

Appendix A. Supplementary data

Supplementary data associated with this article can be found, in the online version, at http://dx.doi.org/10.1016/j.aca.2012.11.030.

References

[1] G.A. Diaz-Quijada, R. Peytavi, A. Nantel, E. Roy, M.G. Bergeron, M.M. Dumoulin, T. Veres, Lab Chip 7 (2007) 856.
[2] C. Jonsson, M. Aronsson, G. Rundstrom, C. Pettersson, I. Mendel-Hartvig, J. Bakker, E. Martinsson, B. Liedberg, B. MacCraith, O. Ohman, J. Melin, Lab Chip 8 (2008) 1191.
[3] P.S. Nunes, P.D. Ohlsson, O. Ordeig, J.P. Kutter, Microfluid. Nanofluid. 9 (2010) 145.
[4] M. Madou, J. Zoval, G.Y. Jia, H. Kido, J. Kim, N. Kim, Annu. Rev. Biomed. Eng. 8 (2006) 601.
[5] J. Ducree, S. Haeberle, S. Lutz, S. Pausch, F. von Stetten, R. Zengerle, J. Micromech. Microeng. 17 (2007) S103.
[6] Y.K. Cho, R. Gorkin, J. Park, J. Siegrist, M. Amasia, B.S. Lee, J.M. Park, J. Kim, H. Kim, M. Madou, Lab Chip 10 (2010) 1758.
[7] R. Peytavi, F.R. Raymond, D. Gagne, F.J. Picard, G. Jia, J. Zoval, M. Madou, K. Boissinot, M. Boissinot, L. Bissonnette, M. Ouellette, M.G. Bergeron, Clin. Chem. 51 (2005) 1836.
[8] R.P. Gandhiraman, C. Volcke, V. Gubala, C. Doyle, L. Basabe-Desmonts, C. Dotzler, M.F. Toney, M. Iacono, R.I. Nooney, S. Daniels, B. James, D.E. Williams, J. Mater. Chem. 20 (2010) 4116.
[9] N.C.H. Le, V. Gubala, R.P. Gandhiraman, S. Daniels, D.E. Williams, Langmuir 27 (2011) 9043.
[10] I.K. Dimov, L. Basabe-Desmonts, J.L. Garcia-Cordero, B.M. Ross, Y. Park, A.J. Ricco, L.P. Lee, Lab Chip 11 (2011) 4279.
[11] J. Siegrist, R. Gorkin, M. Bastien, G. Stewart, R. Peytavi, H. Kido, M. Bergeron, M. Madou, Lab Chip 10 (2010) 363.
[12] D.A. Bartholomeusz, R.W. Boutte, J.D. Andrade, J. Microelectromech. Syst. 14 (2005) 1364.
[13] C.C. O'Mahony, V. Gubala, R.P. Gandhiraman, S. Daniels, J.S. Yuk, B.D. MacCraith, D.E. Williams, J. Biomed. Mater. Res. A 100A (2012) 230.
[14] M. Grumann, A. Geipel, L. Riegger, R. Zengerle, J. Ducree, Lab Chip 5 (2005) 560.
[15] V. Gubala, R.P. Gandhiraman, C. Volcke, C. Doyle, C. Coyle, B. James, S. Daniels, D.E. Williams, Analyst 135 (2010) 1375.
[16] S.R. Ge, K. Kojio, A. Takahara, T. Kajiyama, J. Biomater. Sci.: Polym. Ed. 9 (1998) 131.
[17] J.Y. Yoon, H.Y. Park, J.H. Kim, W.S. Kim, J. Colloid Interface Sci. 177 (1996) 613.
[18] H. Ayhan, J. Bioact. Compat. Polym. 17 (2002) 271.
[19] F.L.G. Flecha, V. Levi, Biochem. Mol. Biol. Educ. 31 (2003) 319.
[20] A. Valsesia, P. Colpo, T. Meziani, F. Bretagnol, M. Lejeune, F. Rossi, A. Bouma, M. Garcia-Parajo, Adv. Funct. Mater. 16 (2006) 1242.
[21] P. Wu, D.G. Castner, D.W. Grainger, J. Biomater. Sci.: Polym. Ed. 19 (2008) 725.
[22] C. Neils, Z. Tyree, B. Finlayson, A. Folch, Lab Chip 4 (2004) 342.
[23] J.Y. Kang, C. Kim, K. Lee, J.H. Kim, K.S. Shin, K.J. Lee, T.S. Kim, Lab Chip 8 (2008) 473.
[24] O. Strohmeier, M. Rombach, D. Mark, R. Zengerle, G. Roth, F.v. Stetten, Proc. of Transducers (2011).